Article

Response of Soil Moisture to Long-Duration Rainstorms in Three Forest Stands in Mountainous Areas of North China

Xuhui Tong [1],* , **Xinlei Ren [2,3,4]** and **Yu Chen [2,3,4]**

1   Geological Survey of Gansu Province, Lanzhou 730000, China
2   College of Forestry, Central South University of Forestry & Technology, Changsha 410004, China
3   Hunan Lutou Forest Ecosystem National Orientation Observation and Research Station,
     Yueyang 414000, China
4   Key Laboratory of Soil and Water Conservation and Desertification Combating, Ministry of Education,
     Changsha 410004, China
*   Correspondence: martintong8856@163.com

Abstract: Rainfall is one of the core components of the water cycle in terrestrial ecosystems and is closely related to hydrothermal balance, plant and animal growth, and stability of the whole ecosystem. Long-duration rainstorms can alter the soil structure of forest ecosystems and affect the spatial distribution of soil moisture, thus affecting the water supply from the soil to trees and being one of the factors that increase the vulnerability of forest ecosystems. In recent years, changes in rainfall patterns have normalized prolonged heavy rainfall in the mountainous areas of North China. However, there are few reports on the response of soil water at different depths to historically long rainstorms in forested areas. By quantifying the relationship between precipitation characteristics and soil water, the soil water transport patterns of *Platycladus orientalis* (*PO*), *Quercus variabilis* (*QV*) and *Pinus tabuliformis* (*PT*) during the long-duration rainstorms of 21–22 July 2012 were evaluated separately, and the roles of different plants in response to the historically long rainstorm were determined. The results showed that (1) the response of different forest stands to rainfall had a lag. Among them, the soil water of *PO* and *PT* were less affected by rainfall and could maintain a relatively stable state. (2) The soil moisture transport trend of *PO* was significantly greater than that of other vegetation zones and covered the whole process of rainfall. Under the three typical vegetation covers, there was a continuous zero-flux plane in the soil at each observed depth (the direction of soil moisture flow is more stable over the rainfall period), but there was no regular transport trend. (3) The root system was an important factor, influencing the differences in soil moisture response of the three vegetation types. *QV* had a higher average effective water recharge rate than lateral cypress and oleander and could better utilize the water recharge from storm water.

Keywords: long-duration rainstorm; soil water content; soil water potential; soil water transport

---

1. Introduction

Soil moisture is an important parameter in the water cycle of terrestrial ecosystems [1–3] that determines soil evolution and land productivity and is also an important influence on soil erosion processes, plant growth, and vegetation recovery [4]. In the groundwater–soil–vegetation–atmosphere continuum (GSPAC) water cycle of forest ecosystems, soil water movement is a key link between water transformation processes at all levels [5,6] and is a key factor affecting forest water retention [4] and soil [7] and vegetation recovery [8].

Soil moisture is closely related to precipitation processes, and precipitation is an important factor that directly affects soil moisture distribution [9] and vegetation water use patterns [8]; the impact of precipitation on ecosystems is also mainly realized through changes in soil moisture, which regulates the structure and function of ecosystems. Soil moisture changes further regulate ecosystem structure and function [6]. There have been many reports on the response of soil moisture to land use, topography, and vegetation

type [5,7,10]. At the same time, it has been found that soil moisture varies with rainfall amount, seasonal variation of rainfall, rainfall ephemeris, rainfall intensity, and rainfall frequency, i.e., there is spatial and temporal heterogeneity of soil moisture response to rainfall [11]. Studies found that the above factors together influence rainfall infiltration and, in turn, soil moisture replenishment in different soil layers [12–14]. In arid and semi-arid regions, changes in soil moisture status (as one of the main influencing factors of terrestrial ecosystems) due to precipitation changes are bound to have a significant impact on ecosystem structure and function [12]. The quantitative analysis of water response factors of water loss through evapotranspiration in arid and semi-arid regions is important for revealing the dynamic changes in soil water and their causes, designing effective management plans for efficient use of water resources, and providing important theoretical support for in-depth exploration of water transport patterns in forest ecosystems [15]. Therefore, it is of great scientific significance and practical value to study the soil moisture transport patterns of forest vegetation under extreme rainfall conditions, especially the characteristics of soil moisture dynamics under the influence of different vegetation types and their response to rainfall, in order to improve the water retention capacity of forest soil.

It was predicted that under the background of global climate change, the occurrence of precipitation and extreme precipitation events in the northern region of China would increase [16]. North China is a semi-arid region, and precipitation in North China had been decreasing year by year since 1950 [17]. At the same time, due to rapid economic development and increasing population, the water demand in North China had increased rapidly compared to the past decades [18]. In this case, the water cycle process will also be significantly altered with the change in vegetation growth and precipitation pattern, and how to improve soil water storage and water use efficiency has become a hot issue in scientific research in recent years [19,20]. High-intensity storm events can produce severe soil erosion, altering soil structure and the spatial distribution of soil water [21–23]. As a functional area for water storage, it was particularly important to study the dynamics of soil water in forest soils during rainfall. Therefore, it was important to accurately analyze and predict the moisture content of different depths of the soil layer at smaller timescales for typical rainstorm processes of high intensity. Previous studies had focused on the full variation of soil water in terms of daily variation, monthly variation, or longer periods [24,25], but there were few reports on the processes of rainfall response to changes in water content and water potential of soil layers at different depths during heavy rainfall.

The North China Mountains are not only an important ecological barrier for Beijing, but also an important link in the ecological barrier of the entire North China Plain, and it is of great significance to study soil moisture transportation and vegetation water use regulation in the mountainous area for in-depth understanding of the water cycle of the North China Plain under a changing environment. Based on field observation by the forest ecological positioning station in the capital circle, the soil moisture movement process of these three typical forest ecosystems under long-duration rainstorms was studied, and the response relationship of soil moisture movement was used to further reveal the regulation of soil moisture movement in forest ecosystems under long-duration rainstorms, which provided a scientific basis for the construction of ecological function-oriented forest vegetation in the region.

2. Materials and Methods

2.1. Study Site Description

The study area was located at the Ecosystem Positioning Station in Jiu Feng National Forestry Park, Haidian District, 30 km northwest of Beijing, China (39°54′ N, 116°28′ E) (Figure 1). The test site had a slope of 10–25° and an average elevation of 140 m. The climate was semi-arid and semi-humid, with an annual mean temperature of 9 °C and multi-year mean precipitation of 600 mm, of which July-September accounts for more than 80% of the annual precipitation.
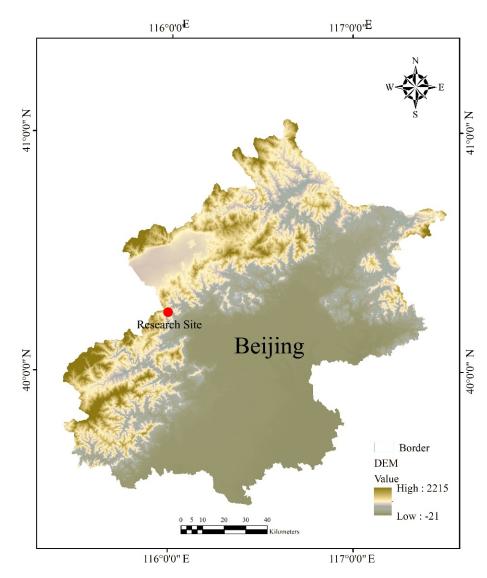
Figure 1. Location map of ecological positioning stations.

Through a survey of the dominant tree species stands in the Jiu Feng National Forestry Park, it was found that the most widely distributed plantations in the forest were cork oak, cypress and oleander (Table 1). Therefore, this paper selects the well-grown *Platycladus orientalis* (*PO*), *Quercus variabilis* (*QV*), and *Pinus tabuliformis* (*PT*) in the forest to establish fixed test plots for experimental observation. The tree species in the three sample plots were in the same period of forestation, and the soil type was coarse, bone-dry brown soil.

Table 1. Overview of the test site.

Stand Type	Longitude, Latitude	Elevation (m)	Major Understory Shrubs	Average Thickness of Litterfall (cm)	Size Plot Sample (m × m)
PO	40°3.766′ N 116°5.750′ E	145	*Vitex negundo*, *Grewia biloba*	4.2 ± 0.9	40 × 40
QV	40°3.511′ N 116°5.242′ E	430	*Vitex negundo*, *Myripnois dioica*	5.1 ± 0.5	40 × 30
PT	40°3.508′ N 116°5.354′ E	395	*Grewia biloba*, *Vitex negundo*	7.2 ± 1.3	60 × 60

2.2. Methods

2.2.1. Precipitation Monitoring

The time period for this study was from 21 July 2012 at 10:30 to 22 July 2012 at 10:30. Precipitation monitoring was mainly carried out using tipping-bucket rainfall barrels for long-term continuous recording. In the open areas near *PT*, *PO*, and *QV* sample plots, two tipping-bucket rainfall barrels were positioned, with an accuracy of 0.2 mm using a HOBO rain gauge (S-RGA-M002, Onset, Bourne, MA, USA). The rainfall was recorded automatically at 10 min intervals. The monitoring results show that 164.4 mm of precipitation fell in a 24 h period. The main precipitation was concentrated between 13:20 and 18:20 on 21 July. The amount of precipitation during this period was 117.2 mm, accounting for 71.3% of the total precipitation in a 16 h period. The average age, maximum and minimum precipitation intensities were 23.4, 46.8, and 12.0 mm/h respectively.

2.2.2. Soil Moisture Content Measurement

Lysimeters were deployed in three stand samples and the soil water content was determined by inserting a measuring probe (ECH$_2$O-TE System, Decagon Devices, Pullman, WA, USA) into the soil at different depths (20 cm, 40 cm, 60 cm, 80 cm, 100 cm, 120 cm, and 160 cm) and recording every 10 min. The surface area of the evapotranspiration meter was 4 m^2 (2 m $\times$ 2 m), the depth was 2.3 m, and the accuracy was 0.01 mm. The same tree species were planted around the evapotranspiration meter to simulate a pure stand environment with a stand density of 2500 plants/ha. The lysimeter contained an electronic balance and a pressure transducer to determine the weight according to the lever principle and to derive the change in water evaporation and water infiltration according to the water balance equation

$$P = ET + R + Q \pm \Delta W \tag{1}$$

where P was the amount of precipitation (mm); ET was evaporation (mm); R was runoff (mm); Q was infiltration (mm); and ΔW the amount of change in weight of the lysimeter (mm). Since the relative humidity during the storm exceeded 99% and the location where the lysimeter was installed was flat with no slope, the values of ET and R can be identified as zero.

2.2.3. Soil Water Potential Measurement

To avoid the impact of canopy-interception rain on the measurement results, we chose to excavate the soil profile in the field without leaf cover, while ensuring that the damage to the original environment was minimized, and 5TE probes and soil water potential probes were placed at 20 cm, 40 cm, 60 cm, 80 cm, 100 cm, 120 cm, and 160 cm depths, with EM50 digital acquisition; the measurement frequency was every 10 min, and continuous measurements were used to monitor soil temperature, soil water content, soil conductivity, and soil water potential at different depths. The soil water potential gradient between two adjacent soil layers was calculated as follows:

$$\psi' = \frac{\psi_2 - \psi_1}{d_2 - d_1} \tag{2}$$

where, ψ_1 and ψ_2 were the upper and lower soil water potential (based on the surface, upward is positive); d_1 and d_2 were the upper and lower depths, respectively; ψ' was the water potential gradient between the two adjacent layers. Positive values represented the lower layer of soil water potential as higher than the upper layer, soil water transport upward, and negative values to the contrary. The horizontal surface where the water potential gradient was zero, i.e., the soil water flux was zero, was called the zero-flux plane. The zero-flux plane method was an important method to study the infiltration of rainfall, irrigation, etc. to recharge soil water and infiltration as well as soil evaporation and infiltration depletion [26]. The extreme value points of the soil water potential distribution curve were divided into two types: maximum value points and minimal value points, and

therefore the zero-flux planes were divided into polymeric and divergent zero-flux planes. The divergent zero-flux plane was located at the maximum value point of the soil water potential distribution curve, above which the soil water moves upward and below which it moves downward. The polymeric zero-flux plane was located at the minimal value point of the soil water potential distribution curve, above which soil moisture moves upward and below which soil moisture moves downward.

3. Results

3.1. Characteristics of Dynamic Changes in Soil Water Content in Forest Land

During the rainstorm, the overall trend of soil water content change in the three forest stands was the same, mainly divided into three phases: lagging, rising, and receding, but the degree of change also varied among different forest stands (Figure 2). At the initial stage of rainfall, i.e., within the first 3 h of rainfall, the soil moisture content in the three stands remained stable, with the lag time of moisture in the top soil layer (0–20 cm) of each stand from short to long: *PO* (100 min), *QV* (190 min), *PT* (200 min). However, at the 4th hour of rainfall, rainwater rapidly infiltrated to 40 cm under *PO*, 40 cm under *QV*, and 60 cm under *PT*, and the water content of the corresponding soil layers increased extremely rapidly. After 4 h of rainfall, the soil water content of each stand below the 80 cm soil layer also increased significantly, but the increment was significantly lower than that of the shallow soil layer and the response interval was longer, which showed that the heavy rainfall had no significant effect on the deep soil water recharge of *QV*. After 18:20 on 21 July, the rainfall decreased significantly and the water content of each soil layer also decreased; it can be seen that the rate of water content decrease in the shallow soil layer (0−80 cm) was higher than that in the deep soil layer (80–100 cm).
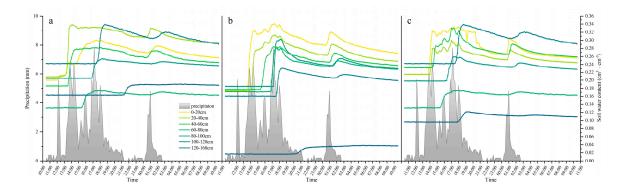

Figure 2. Dynamics of soil water content in different stands (where (**a**) was a *PO* stand, (**b**) was a *QV* stand, and (**c**) was a *PT* stand).

3.2. Characteristics of Soil Moisture Changes at Different Depths in Woodlands

The value of the soil moisture coefficient of variation reflected the stability of soil moisture. The lower the value, the less soil moisture was affected by precipitation and other factors and could maintain a relatively stable state, while the higher the value, the more active the soil moisture was, and the magnitude of variation was large. During heavy rainfall, the soil moisture content of each layer changed dramatically (Table 2), with *PT* and *PO* variability coefficients (CV) almost similar, distributed between 0.070–0.120, while *QV* had the highest coefficient of variation at 0.120–0.350. The absolute variability (extreme difference) of soil water content was *QV* (0.168) > *PO* (0.130) > *PT* (0.118). The magnitude of variation and coefficient of variation of the soil water content for different vegetation showed a gradual decrease with depth. *QV* had the smallest water content in the 120–160 cm soil layer, and there was a clear break in water content of the soil layer above 120 cm; the variation was also the smallest among the three forest stands. Therefore, the soil water under the cover of *QV* had difficulty infiltrating into the soil layer below 120 cm, and the rainfall had a weak effect on the recharge of groundwater in this stand.

Table 2. Characteristics of soil water content changes in different soil layers.

Forest Stand Type	Depth (cm)	Maximum Value	Minimum Value	Difference	Standard Deviation	Coefficient of Variation
PO	0–20	0.300	0.200	0.100	0.027	0.100
	20–40	0.338	0.208	0.130	0.037	0.123
	40–60	0.282	0.186	0.096	0.029	0.114
	60–80	0.175	0.131	0.044	0.015	0.093
	80–100	0.254	0.205	0.049	0.018	0.076
	100–120	0.339	0.241	0.098	0.034	0.117
	120–160	0.191	0.162	0.029	0.013	0.073
QV	0–20	0.341	0.173	0.168	0.047	0.167
	20–40	0.313	0.174	0.139	0.039	0.153
	40–60	0.284	0.176	0.108	0.034	0.142
	60–80	0.280	0.171	0.109	0.033	0.149
	80–100	0.302	0.184	0.118	0.032	0.139
	100–120	0.231	0.160	0.071	0.024	0.124
	120–160	0.039	0.017	0.022	0.010	0.350
PT	0–20	0.332	0.214	0.118	0.035	0.127
	20–40	0.299	0.215	0.084	0.021	0.082
	40–60	0.330	0.232	0.098	0.024	0.087
	60–80	0.175	0.131	0.044	0.015	0.093
	80–100	0.259	0.198	0.061	0.019	0.083
	100–120	0.339	0.241	0.098	0.034	0.117
	120–160	0.121	0.096	0.025	0.008	0.077

3.3. Characteristics of Soil Water Potential Dynamics in Forest Land

During the experiment, the water potential of the soil layer at different depths in each stand changed accordingly (Figure 3). During the heavy rainfall, the soil water potential in the 0–40 cm soil layer of the three stands changed more significantly during the third hour of rainfall, and the water potential in the 60 cm soil layer also started to rise rapidly from the fourth hour of rainfall; this result was the same as the change in soil water content. The water in the 0–60 cm soil layer of the three stands was close to saturation 5 h later, and the water potential remained around −12 Kpa. The water potential in the 160 cm soil layer remained relatively saturated during the rainfall period (water potential ranged from −9 to −19 Kpa), except for *QV*, where the water potential in the 160 cm soil layer under the forest changed drastically during the 10th hour of rainfall, from −197 to −12 Kpa. The effect of heavy rain on the deep soil moisture recharge of *QV* was not obvious, and the water content of the soil layer was low before rainfall, which may have been due to the lack of soil moisture and insufficient rainfall, making it difficult for soil moisture to reach the deep soil by down-filtration and recharge the water.
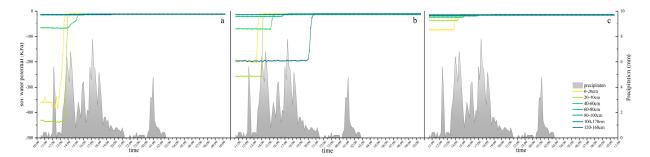

Figure 3. Dynamics of soil water potential in different stands. (Where (**a**) was a *PO* stand, (**b**) was a *QV* stand, and (**c**) was a *PT* stand.).

3.4. Characteristics of Soil Water Potential Gradient and Zero-Flux Plane Changes in Forest Land

The soil water potential gradient at the adjacent observation depths of different vegetation monitoring sites during the long-duration rainstorm varied, and the absolute value of the 0–80 cm water potential gradient of *PO* was significantly larger than that of other vegetation zones, with a maximum value of 18.53 kPa/cm, and was maintained throughout the rainfall (Figure 4). This indicates that the shallow soil water in *PO* had a continuous tendency to transport more water during the rainfall. The soil water potential gradient at different depths of *QV* only showed large absolute values during the first half of the rainfall period (10:30–22:30), and gradually tended to zero with increasing rainfall time. The absolute maximum value of the soil water potential gradient in the area covered by *PT* was only 1.85 kPa/cm at the beginning of the rainfall period, and then gradually decreased with the increase of rainfall time. variabilis Blume cover only had a greater effect at the beginning of the rainfall, and the greatest effect was on *PO* cover.
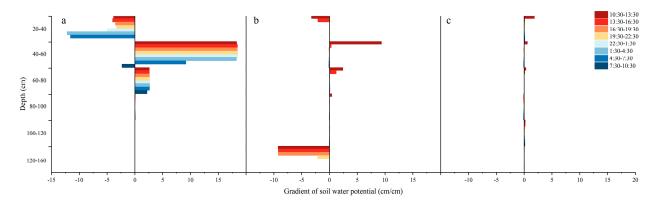

Figure 4. Changes in soil water potential gradient under different vegetation types ((**a**) *PO* stands, (**b**) *QV* stands, and (**c**) *PT* stands, where the water potential gradient was negative when the deep soil water potential was lower than the shallow soil water potential, and positive when vice versa).

According to the changes in the location of the soil moisture zero-flux plane, the direction of moisture transport in the soil profile under the three typical vegetation covers changed, and a persistent zero-flux plane existed at all observed depths (Figure 5). After rainfall, the polymeric zero-flux plane moved down to 60 cm from 40 cm and the divergent zero-flux plane appeared at 40 cm. The polymeric zero-flux plane existed only at 40 cm in the soil of the covered area during the first 2 h of rainfall, and then this zero-flux plane kept descending and finally stabilized at 60 cm and 120 cm. During the 2nd and 6th hours of rainfall, the soil in the *QV* cover area showed a continuous divergent zero-flux plane at a depth of 120 cm and 40 cm, respectively, and with the increase of rainfall time, the divergent zero-flux plane at 120 cm finally stabilized at 100 cm. Before the rainfall, the divergent zero-flux plane and polymeric zero-flux plane existed in *PT* covering soil at 80 cm and 100 cm depth, respectively. In addition, a continuous divergent zero-flux plane was observed in *PT*-covered soil at a depth of 40 cm after 4 h of rainfall.
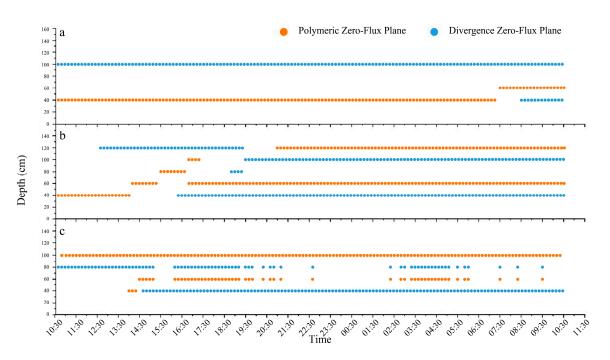
Figure 5. Changes in zero-flux surface location under different vegetation types ((**a**) *PO* stands, (**b**) *QV* stands, and (**c**) *PT* stands).

4. Discussion

Compared with previous studies on soil moisture transport trends and fluxes influenced by rainfall at monthly and annual scales [20], there were differences in soil moisture transport patterns at different timescales. The response of precipitation infiltration was the dominant factor in the short timescale, while the long timescale was the result of a combination of factors such as precipitation recharge, soil evaporation, and vegetation transpiration. Therefore, rainfall at the daily scale did not cause a regular zero-flux upward or downward shift, probably due to the interception of rainfall by the canopy and deadfall after more than a decade of vegetation growth [27,28] and the influence of the root system on soil structure [15,29,30], which changed the soil water transport mechanism to some extent, resulting in different degrees of soil water recharge at all depths in a relatively short period of time of recharge [31] (Figure 6). Therefore, in order to further investigate the influence of root systems on the difference in soil water response in the three forest stands, we conducted field survey sampling of plant root systems of three tree species, *PO*, *QV*, and *PT*, integrated the distribution of the three root systems, and statistically found that *PO* roots were mainly distributed between 0–40 cm of soil, *QV* roots were mainly distributed between 0–60 cm of soil and *PT* roots were mainly distributed between 20–60 cm of soil. It could be seen that during rainfall, a continuous aggregated zero-flux surface occurred at all three woodland soil root locations, resulting in the presence of preferential flow within the soil profile. Therefore, when heavy rainfall occurred, the preferential flow would rapidly recharge downward, resulting in a higher recharge rate from the deeper soils than the shallow soils. This phenomenon has also been confirmed in other relevant studies [31,32].

Rainfall is the main source of water recharge for vegetation growth in the region, and the amount of rainfall is a decisive factor affecting the depth of shallow soil water recharge [33]. However, heavy rainfall decreased the effective recharge rate of soil moisture, and the effective recharge efficiency of soil moisture differed among vegetation under heavy rainfall conditions [34,35]. Since the rainfall monitoring sites in this study were all located in open areas near each vegetation cover, there were no significant differences in the amount of penetrating rainfall under different vegetation covers, although there were some differences in the canopy interception of each vegetation. Therefore, we judged the effective recharge rate of stormwater to the soil of the three forest stands by directly

comparing the maximum value of the increase in soil water content of each soil layer in the three stands (Table 3). We found that the soil texture in the area around the root distribution was loose, and the porosity of its shallow soil increased with the growth cycle, which led to a significant recharge effect in the main root distribution area in the lower layer of the soil profile, where the average effective water recharge rate of *QV* was higher than that of *PO* and *PT*.
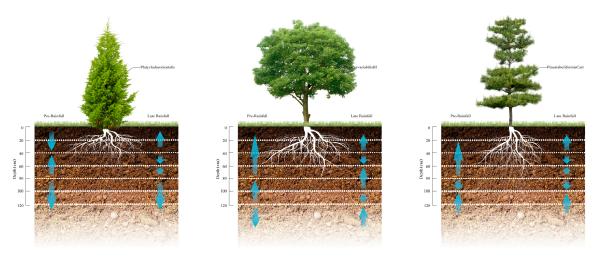

Figure 6. Soil water transport pattern under different vegetation type covers.

Table 3. Maximum increase in soil water content under different vegetation types.

	0–20 cm	20–40 cm	40–60 cm	60–80 cm	80–100 cm	100–120 cm	120–160 cm	Average Value
PO	0.10	0.13	0.10	0.04	0.05	0.10	0.03	0.08
QV	0.17	0.14	0.11	0.11	0.12	0.07	0.02	0.10
PT	0.12	0.08	0.10	0.04	0.06	0.10	0.02	0.08

5. Conclusions

Based on the observation data of soil water content and water potential dynamics under the cover of typical plantation vegetation (*PO*, *QV*, *PT*) in the mountainous areas of North China during the long-duration, extraordinarily heavy rainfall on 21–22 July 2012, main conclusions from our analysis are as follows:

(1)　The increase in soil water lagged behind the increase in rainfall, which indicated that for different forest stands there was a lag in response to rainfall. In comparison, *PO* had the shortest response time, while *PT* had the longest response time. It can be seen that the soil in the surface layer of *PO* has the greatest porosity, the soil is softer, and it is more conducive to the rapid infiltration of rainwater. The effect of rainfall on the water replenishment of the deep soil for *QV* is not obvious, and it can be seen that the rainfall is insufficient and penetrates into the deep soil for water replenishment, which shows that the deep soil texture of *QV* is harder. The coefficient of variation for soil moisture content for the two conifers was smaller than that of *QV*, which showed that the soil moisture of the two conifers was less influenced by precipitation and other factors and can maintain a relatively stable state with little variation.

(2)　The variations in soil moisture transport trends in the soil profiles under three typical vegetation covers during long-duration rainstorms were different. *QV* showed a greater moisture transport trend only in the first half of the rainfall period (10:30–22:30), while *PT* covered the area with the smallest soil water potential gradient. Persistent zero-flux surfaces were present in the soils at all observed depths under the three typical vegetation covers during the rainfall period. None of the soil profiles showed a regular trend of movement in the direction of water transport.

(3)　　The root system was an important factor influencing the difference in soil moisture response in the three stands, and the preferential flow of water was rapidly recharged to the root range. Among them, *QV* had a higher average effective water recharge rate than *PO* and *PT*, which could better utilize the water recharge brought by heavy rainfall.

References

1.　Bindlish, R.; Jackson, T.J.; Wood, E.; Gao, H.; Starks, P.; Bosch, D.; Lakshmi, V. Soil moisture estimates from TRMM Microwave Imager observations over the Southern United States. *Remote Sens. Environ.* **2003**, *85*, 507–515. [CrossRef]

2.　Song, D.; Zhao, K.; Guan, Z. Advances in research on soil moisture by microwave remote sensing in China. *Chin. Geogr. Sci.* **2007**, *17*, 186–191. [CrossRef]

3.　Kray, J.A.; Cooper, D.J.; Sanderson, J.S. Groundwater use by native plants in response to changes in precipitation in an intermountain basin. *J. Arid Environ.* **2012**, *83*, 25–34. [CrossRef]

4.　Li, S.; Deng, W.-Z.; Li, J.; Tao, H.-Z.; Gan, L. Effect of tillage on soil moisture and rainfall response mechanism in Karst Areas of Guangxi. *Water Sav. Irrig.* **2021**, *6*, 31–36.

5.　He, Z.-B.; Zhao, W.-Z. Variability of Soil Moisture of Shifting Sandy Land and Its Dependence on Precipitation in Semi-arid Region. *J. Desert Res.* **2002**, *22*, 359.

6.　Harper, C.W.; Blair, J.M.; Fay, P.A.; Knapp, A.K.; Carlisle, J.D. Increased rainfall variability and reduced rainfall amount decreases soil CO_2 flux in a grassland ecosystem. *Glob. Change Biol.* **2010**, *11*, 322–334. [CrossRef]

7.　Van Rheenen, J.W.; Werger, M.J.A.; Bobbink, R.; Daniels, F.J.A.; Mulders, W.H.M. Short-term accumulation of organic matter and nutrient contents in two dry sand ecosystems. *Vegetatio* **1995**, *120*, 161–171. [CrossRef]

8.　Liu, Z.Q.; Yu, X.X.; Lou, Y.H.; Li, H.Z.; Jia, G.D.; Lu, W.W. Water use strategy of Platycladus orientalis in Beijing mountainous area. *Acta Ecol. Sin.* **2017**, *37*, 3697–3705.

9.　Cheng, R.R.; Chen, Q.W.; Zhang, J.G.; Shi, W.Y.; Li, G.; Du, S. Soil moisture variations in response to precipitation in different vegetation types: A multi-year study in the loess hilly region in China. *Ecohydrology* **2020**, *13*, e2196. [CrossRef]

10.　Wilson, S.D.; Kleb, H.R. The Influence of Prairie and Forest Vegetation on Soil Moisture and Available Nitrogen. *Am. Midl. Nat.* **1996**, *136*, 222–231. [CrossRef]

11.　Wilson, D.J.; Western, A.W.; Grayson, R.B. Identifying and quantifying sources of variability in temporal and spatial soil moisture observations. *Water Resour. Res.* **2004**, *40*, 191–201. [CrossRef]

12.　Chen, M.L.; Zhang, B.W.; Ren, T.T.; Wang, S.S.; Chen, S.P. Responses of soil moisture to precipitation pattern change in semiarid grasslands in Nei Mongol, China. *Chin. J. Plant Ecol.* **2016**, *40*, 658–668.

13.　Wang, H.; Hou, Q.; Feng, X.; Yun, W. Effect of Different Magnitude Rainfall Process on Soil Moisture in Typical Grassland of Xilinhot of Inner Mongolia. *J. Arid. Meteor.* **2016**, *34*, 1010.

14.　Li, X.; Wu, B.; Zhang, J.; Xin, Z.; Dong, X.; Duan, R. Dynamics of shallow soil water content in Nitraria tangutorum nebkha and response to rainfall. *Acta Ecol. Sin.* **2019**, *39*, 1–8.

15.　Cai, G.C.; Ahmed, M.A.; Abdalla, M.; Carminati, A. Root hydraulic phenotypes impacting water uptake in drying soils. *Plant Cell Environ.* **2022**, *45*, 650–663. [CrossRef]

16.　Su, B.D.; Jiang, T.; Jin, W.B. Recent trends in observed temperature and precipitation extremes in the Yangtze River basin, China. *Theor. Appl. Climatol.* **2006**, *83*, 139–151. [CrossRef]

17.　Huang, J.; Sun, S.; Xue, Y.; Zhang, J. Spatial and temporal variability of precipitation indices during 1961–2010 in Hunan Province, central south China. *Theor. Appl. Climatol.* **2014**, *118*, 581–595. [CrossRef]

18.　Wu, P.L.; Zhang, W. Water crisis and sustainable water resource utilization in Beijing. *J. Liaoning Tech. Univ.* **2005**, *24*, 436–439.

19.　Scharwies, J.D.; Dinneny, J.R. Water transport, perception, and response in plants. *J. Plant Res.* **2019**, *132*, 311–324. [CrossRef]

20. Li, Y.R.; Ma, Y.; Song, X.F.; Yang, L.H.; Liu, E.M.; Wang, S.B.; Wang, J. Soil water potential dynamics and water utilization of typical planted forests in the mountain area of North China. *Acta Ecol. Sin.* **2021**, *41*, 5622–5631.

21. González-Hidalgo, J.C.; Peña-Monné, J.L.; Luis, M.D. A review of daily soil erosionin Western Mediterranean areas. *Catena* **2007**, *71*, 193–199. [CrossRef]

22. Zhu, T.X. Effectiveness of conservation measures in reducing runoff and soil loss under different magnitude-frequency storms at plot and catchment scales in the semiarid agricultural landscape. *Environ. Manag.* **2016**, *57*, 671–682. [CrossRef] [PubMed]

23. Destro, E.; Amponsah, W.; Nikolopoulos, E.I.; Marchi, L.; Marra, F.; Zoccatelli, D.; Borga, M. Coupled prediction of flash flood response and debris flow occurrence:application on an alpine extreme flood event. *J. Hydrol.* **2018**, *558*, 225–237. [CrossRef]

24. Sánchez, N.; Martínez-Fernández, J.; González-Piqueras, J.; González-Dugo, M.P.; Baroncini-Turrichia, G.; Torres, E.; Calera, A.; Pérez-Gutiérrez, C. Water balance at plot scale for soil moisture estimation using vegetation parameters. *Agric. For. Meteorol.* **2012**, *166–167*, 1–9. [CrossRef]

25. Jia, X.; Shao, M.A.; Wei, X.; Wang, Y. Hillslope scale temporal stability of soil water storage in diverse soil layers. *J. Hydrol.* **2013**, *498*, 254–264. [CrossRef]

26. Yang, C.; Sakai, M.; Jones, S.B. Inverse method for simultaneous determination of soil water flux density and thermal properties with a penta-needle heat pulse probe. *Water Resour. Res.* **2013**, *49*, 5851–5864. [CrossRef]

27. Mccune, D.C.; Boyce, R.L. Precipitation and the transfer of water, nutrients and pollutants in tree canopies. *Trends Ecol. Evol.* **1992**, *7*, 4–7. [CrossRef]

28. Clausnitzer, F.; Köstner, B.; Schwärzel, K.; Bernhofer, C. Relationships between canopy transpiration, atmospheric conditions and soil water availability—Analyses of long-term sap-flow measurements in an old Norway spruce forest at the Ore Mountains/Germany. *Agric. For. Meteorol.* **2011**, *151*, 1023–1034. [CrossRef]

29. Kolb, E.; Legue, V.; Bogeat-Triboulot, M.B. Physical root-soil interactions. *Phys. Biol.* **2017**, *14*, 065004. [CrossRef] [PubMed]

30. Jin, K.; White, P.J.; Whalley, W.R.; Shen, J.; Shi, L. Shaping an Optimal Soil by Root–Soil Interaction. *Trends Plant Sci.* **2017**, *22*, 823–829. [CrossRef]

31. Li, S.L.; Liang, W.L. Spatial-temporal soil water dynamics beneath a tree monitored by tensiometer-time domain reflectometry probes. *Water* **2019**, *11*, 1662. [CrossRef]

32. Lou, S.L.; Liu, M.X.; Yi, J.; Zhang, H.L.; Li, X.F.; Yang, Y.; Wang, Q.Y.; Huang, J.W. Influence of vegetation coverage and topographic position on soil hydrological function in the hillslope of the three gorges area. *Acta Ecol. Sin.* **2019**, *39*, 4844–4854.

33. Jia, J.; Yu, X.; Li, Y. Response of forestland soil water content to heavy rainfall on Beijing Mountain, northern China. *For. Res.* **2016**, *27*, 541–550. [CrossRef]

34. Chen, H.; Zhang, W.; Wang, K.; Fu, W. Soil moisture dynamics under different land uses on karst hillslope in northwest Guangxi, China. *Environ. Earth Sci.* **2010**, *61*, 1105–1111. [CrossRef]

35. Reichert, J.M.; Prevedello, J.; Gubiani, P.I.; Vogelmann, E.S.; Reinert, D.J.; Consensa, C.O.B.; Soares, J.C.W.; Srinivasan, R. Eucalyptus tree stockings effect on water balance and use efficiency in subtropical sandy soil. *For. Ecol. Manag.* **2021**, *497*, 119473. [CrossRef]